Optical Billiards for Atoms

V. Milner, J. L. Hanssen, W. C. Campbell, and M. G. Raizen
Department of Physics, The University of Texas at Austin, Austin, Texas 78712-1081
(Received 7 September 2000)

One of the central paradigms for classical and quantum chaos in conservative systems is the two-dimensional billiard in which particles are confined to a closed region in the plane, undergoing elastic collisions with the walls and free motion in between. We report the first realization of billiards using ultracold atoms bouncing off beams of light. These beams create the desired spatial pattern, forming an "optical billiard." We find excellent agreement between theory and our experimental demonstration of chaotic and stable motion in optical billiards, establishing a new testing ground for classical and quantum chaos.

DOI: 10.1103/PhysRevLett.86.1514 PACS numbers: 05.45.Mt, 03.75.Dg, 42.50.Vk

Billiards have been the subject of active research in physics and mathematics for many years [1]. It is well known that the dynamics in this system are governed by the shape of the billiard. For example, particles in a circular billiard move along stable, periodic orbits. In contrast, particle motion in a stadium-shaped billiard is chaotic, with exponential divergence and randomness of trajectories [2]. The renewed interest in billiards in recent years has brought to light a number of fundamental problems in physics, including justification of a probabilistic approach to statistical mechanics, and the existence of Maxwell's demon [2–4]. On the experimental side, billiards have been studied in quantum dots [5,6], microwave cavities [7–9], and were found to be relevant to the design of directional micro-lasers [10]. However, many important issues have not been clearly addressed in these systems. These include the effects of soft boundaries [11], surface scattering [12,13], and particle interactions [14]. Here we present a new experimental system for the study of billiards based on ultracold atoms confined in a spatial structure formed by beams of light. This system offers unique advantages of choosing arbitrary billiard geometry, dynamical changing of parameters, introducing noise and decoherence, and studying the role of quantum and many-body effects. We test the capabilities of optical billiards by measuring atomic motion in different regimes of classical chaos and show an agreement with classical theory and numerical simulations.

To create an optical billiard we use two acousto-optic deflectors (AOD), each one deflecting the laser beam in one of the two orthogonal directions (Fig. 1). By scanning the deflection angles synchronously, an arbitrary two-dimensional light pattern is "drawn" in a plane perpendicular to the optical axis. Laser light of frequency higher than atomic resonance creates a repulsive dipole potential which is proportional to the laser intensity and inversely proportional to the detuning. For a sufficiently rapid scan of the laser beam, this potential is well approximated by a static potential barrier — the billiard wall. This method was used recently to generate a circular rotating-beam optical trap for cold rubidium atoms [15]. In order to confine the atomic motion to two-dimensional planes we add a stationary standing wave along the optical axis. As a result of the repulsive potential, atoms move in planes defined by the nodes of the standing wave and bounce elastically off the scanning billiard beam. The relatively large Rayleigh length of the billiard beam ($\sim$2.7 mm, much bigger than the size of the atomic cloud) ensures the equivalence between many independent two-dimensional billiard regions cut by the standing wave from the three-dimensional light pattern.

In this work we focus on a billiard geometry known as a "symmetric gravitational wedge" first introduced by Lehtihet and Miller [16]. This system consists of a point mass m moving in a constant gravitational field $\mathbf{g}$ between two straight, intersecting, elastic boundaries, which are symmetrically inclined by equal angles to the direction of gravity, forming a two-dimensional wedge that confines the motion (see the lower panels in Fig. 2). Despite a very simple shape, dynamical behavior of the gravitational wedge is amazingly rich and can be tuned from stability

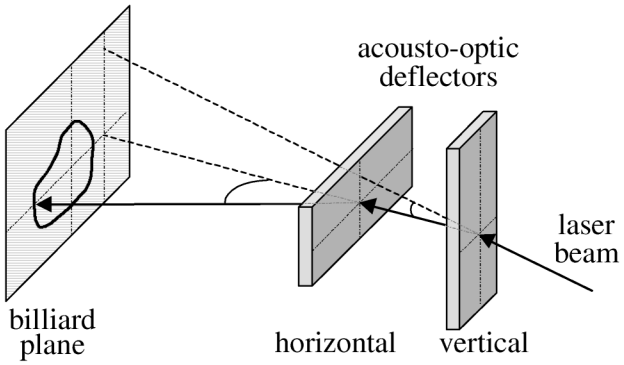

FIG. 1. Simplified scheme of the optical setup. The deflection angles of two acousto-optic devices are controlled by two arbitrary function generators. By scanning these angles synchronously, the desired spatial pattern of light can be "drawn" in the billiard plane (the focal plane of the imaging optics, which is omitted for clarity). An additional standing wave (not shown) is aligned perpendicular to the billiard plane and confines atomic motion to two dimensions.

 0031-9007/01/86(8)/1514(4)$15.00

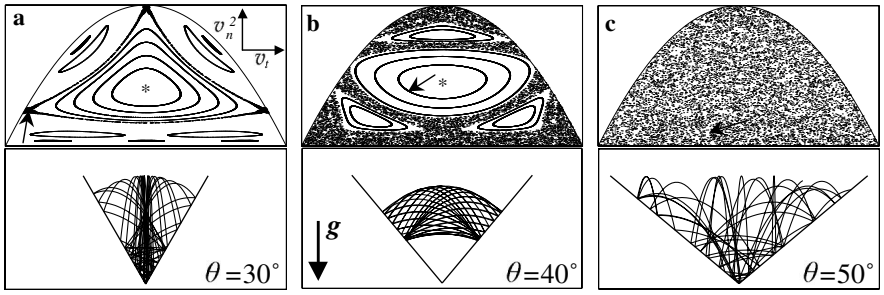

FIG. 2. Poincaré surfaces of a section of the gravitational wedge are plotted in the upper panels for $\theta = 30°$ (a), $\theta = 40°$ (b), and $\theta = 50°$ (c). The axes of the phase space are shown in the top right corner of panel a (see text). For each angle, we show one real-space trajectory (lower panels) starting from the initial conditions marked by an arrow on the corresponding phase space portrait. The trajectory is weakly chaotic in case (a) (i.e., it connects to a very small region of the phase space), periodic in case (b), and fully chaotic in (c) (i.e., it explores the whole phase space). An isolated fixed point corresponding to the dominant periodic orbit of the system is marked by an asterisk in cases (a) and (b).

to chaos with a single parameter—the vertex half-angle θ ($0° < \theta < 90°$).

In order to examine the dynamical properties of the billiard, it is convenient to follow its trajectories in the phase space. The phase space of the gravitational wedge is four dimensional. However, conservation of energy and the fact that all trajectories reach the billiard boundaries make it possible to project the phase space onto a two-dimensional plane—the Poincaré surface of a section, defined by $m\mathbf{v}^2/2 + mgy = E$, $y = x/\tan(\theta)$, where x and y are the spatial coordinates of the particle (the origin is at the wedge vertex) and $\mathbf{v}$ its velocity. In Fig. 2, we plot the square of the normal component of $\mathbf{v}$, v_n^2, versus its tangential component v_t at the points of bounce. When $\theta = 45°$, the motion along the wedge boundaries is separable and therefore completely integrable. Numerical studies [16–18] demonstrate that for $\theta < 45°$ the phase space is mixed. Here, the regions of global chaos coexist with the stable quasiperiodic trajectories, and particle motion depends on the initial conditions. The relative amount of chaos in this regime was shown to oscillate, having its minima at $\theta_n = 90°/n$, $n = 3, 4, 5, \ldots$. For instance, at $\theta = 30°$ only a very weak chaotic component is observed near unstable periodic points, as illustrated in Fig. 2a by an arrow pointing at the small region of confined chaos. Between these special angles θ_n both chaotic and stable structures may occupy comparable areas (Fig. 2b). Here, a simply connected domain of global chaos fills the phase space between the stable orbits. An abrupt change in dynamics occurs above 45°, where the system exhibits hard chaos, and all periodic trajectories become unstable (Fig. 2c).

It is important to emphasize that the reason for the chaos in the gravitational wedge is the singularity of the vertex [18]. Thus, any point in the chaotic sea is necessarily connected with the wedge vertex [the upper domed boundary in the phase space portraits (Fig. 2)]. This important property of the wedge billiard allows us to study its dynamics by measuring the survival probability of a particle in the wedge with a "hole" at the vertex (see Fig. 3). Indeed, particles that are trapped within stable islands do not reach the vertex and therefore cannot fall through the hole. Others, however, sooner or later come arbitrarily close to the vertex and escape from the wedge. This effect is illustrated by a few examples of the periodic and chaotic trajectories in Fig. 2.

Confining atomic motion inside optical billiards requires a source of ultracold atoms. In our experiment, we first trap and cool $\sim 10^6$ cesium atoms in a standard magneto-optical trap (MOT) [19]. Subsequent polarization-gradient cooling yields a temperature of 10 μK with the initial spatial distribution radius of the atomic cloud of 0.2 mm. After turning the trapping fields off, the billiard beam and the standing wave are turned on simultaneously, and the atoms are left in the gravitational wedge for up to 450 ms. The fraction of atoms that remained in the billiard, as well as their spatial distribution, is detected by turning the MOT trapping beams on in zero magnetic field (thus effectively freezing the position of the atoms in optical molasses [19]) and imaging fluorescence in a short (50 ms) exposure on a cooled high-resolution charge-coupled device (CCD) camera.

The billiard and the standing wave beams are provided by a Ti:sapphire laser detuned 1.7 nm above the atomic

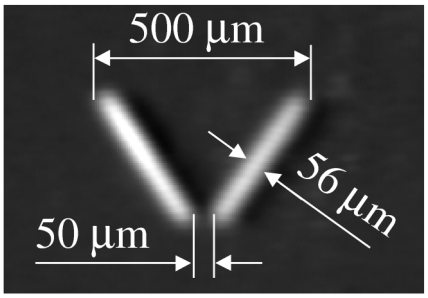

FIG. 3. Picture of the optical wedge with a hole, taken with the CCD camera at the focal plane of the billiard beam. The angle, hole diameter, and intensity distribution may be dynamically varied, while the total size and the beam diameter are determined by the optical setup.

transition of cesium. After passing through the acousto-optic deflectors, the billiard beam is focused into the vacuum chamber and has a $1/e^2$ radius of 28 μm and power of 200 mW. Drawing a hole at a certain location on the billiard wall is achieved by switching off the power of the radio-frequency signal, which controls the diffraction efficiency of the AOD. The size of the billiards is measured independently on a second CCD camera. As shown in Fig. 3, the maximum linear dimension of the wedge is 500 μm. It is much smaller than the 2.6 mm diameter of the standing wave, which makes the two-dimensional motion approximation well justified. The lower billiard edge is positioned 250 ± 50 μm below the center of the MOT and is fixed for all angles θ. In the longitudinal direction, we carefully match the focal plane of the billiard beam with the position of the atomic cloud. In order to create an effectively stationary wall, which is of crucial importance for the regime of specular reflection, one needs to scan the billiard beam as fast as possible. The response time of the acousto-optic deflectors (0.55 μs) limits the scan rate to $\sim$80 KHz. We set the scan rate to 20 KHz, after confirming that the results do not depend upon this parameter at rates higher than 3 KHz.

In Fig. 4 we plot the survival probability in the gravitational wedge with a hole diameter of 75 μm as a function of its half-angle θ. The survival probability is calculated as the number of atoms detected in the billiard after 300 ms and normalized by the initial number of atoms in the wedge. The latter is measured at $t = 25$ ms, when the rest of the atoms, falling due to gravity, are out of the camera's sight. This takes into account the different loading efficiency of atoms into the billiard, which depends on θ due to the comparable sizes of the wedge and the initial atomic cloud. The result clearly demonstrates an expected oscillatory behavior. At $\theta = 22.5°$ and 30°

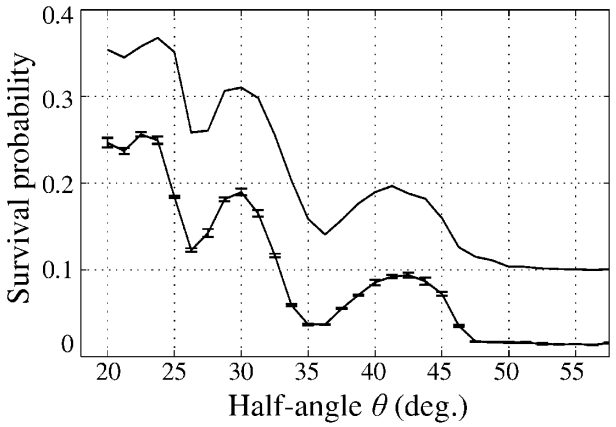

FIG. 4. Survival probability in the gravitational wedge at $t = 300$ ms. Experimental curve is shown with the error bars corresponding to 1 standard deviation. The results of the classical calculations (upper curve) have been divided by 2 and shifted up by 0.1. The calculations have been performed with 10 000 particles. They include wall softness, spontaneous emission, finite size of the billiard, and do not have any fitting parameters.

(90°/4 and 90°/3), the measure of the stable structures in the phase space is at maximum, resulting in a larger amount of trapped atoms. Since all periodic trajectories of the $\theta = 45°$ wedge connect to the vertex, the third peak is shifted towards angles smaller than 45°, where this connection is broken for most of the remaining stable orbits. In exact agreement with theory [17], which predicts complete chaos at $\theta \approx 26°, 34°$, and above 45°, we see distinct minima at these angles. An inherent feature of optical billiards is the softness of the walls due to the finite penetration depth of an atom into the Gaussian profile of the laser beam. In the case of the gravitational wedge, softness results in an effective decreasing of the wedge angle, since the classical turning point is farther from the wall center for higher points of bounce, where the kinetic energy is smaller. This effect results in a shift of all peaks and valleys of the oscillation curve by as much as 10° from their expected locations. We correct for the wall softness by reducing the light intensity linearly with height, such that it decreases to zero at 500 μm from the bottom of the wedge. This correction is not complete, as the penetration depth depends only upon a normal component of atomic velocity. However, one would expect that averaging of the effective angle along each trajectory would result in better angle matching, as indeed was observed in our experiment. To make an exact verification of this assumption, we calculate classical trajectories numerically, where we include initial spatial and momentum distributions of the atomic cloud, real size of the wedge, wall softness, and spontaneous emission. The result of the numerical analysis, shown in Fig. 4, is in excellent agreement with the experimental observation. Although a classical model is sufficient to describe our current results, quantum effects should become important at lower initial temperatures. We attribute the discrepancy (by a factor of $\sim$2) in the overall magnitude of the signal to the elastic collisions between cesium atoms in the billiard, which may enhance the escape rate due to the mixing of trajectories. The effect of interatomic collisions on billiard dynamics is under current investigation. Finally, we have measured the survival probability as a function of time for different wedge angles and have observed nonexponential escape rates from the billiard in the regimes where the dynamics are not fully chaotic. This effect may be due to the complicated hierarchy of stable structures near the primary stability islands and will be the topic of further research.

The ability to choose an arbitrary billiard geometry and vary it dynamically in time, coupled with the techniques for cooling and trapping of atoms, opens many directions for future work. These include the study of quantum effects [20,21], many-body interactions, quantum statistics, and decoherence in chaotic systems. The optical billiard can also be viewed as a novel trap where particle dynamics are controlled by the geometrical shape, providing a new tool in the control of atomic motion.

This work was supported by the National Science Foundation, the R. A. Welch Foundation, the Texas Higher Education Board, and the Sid W. Richardson Foundation. Authors are thankful to W. Oskay and D. Steck for their help in the laboratory and to B. Sundaram and Yu. L. Bolotin for useful discussions.

[1] H.-J. Stöckmann, *Quantum Chaos: An Introduction* (Cambridge University Press, New York, 1999).
[2] G. M. Zaslavsky, Phys. Today **52**, No. 8, 39 (1999).
[3] D. A. Egolf, Science **287**, 101 (2000).
[4] E. J. Heller, in *Chaos and Quantum Physics,* edited by M.-J. Giannoni, A. Voros, and J. Zinn-Justin (Elsevier Science, North-Holland, Amsterdam, 1991).
[5] R. A. Jalabert, H. U. Baranger, and A. D. Stone, Phys. Rev. Lett. **65**, 2442 (1990).
[6] C. M. Marcus *et al.,* Phys. Rev. Lett. **69**, 506 (1992).
[7] E. Doron, U. Smilansky, and A. Frenkel, Phys. Rev. Lett. **65**, 3072 (1990).
[8] H.-J. Stöckmann and J. Stein, Phys. Rev. Lett. **64**, 2215 (1990).
[9] S. Sridhar and E. J. Heller, Phys. Rev. A **46**, R1728 (1992).
[10] J. U. Nöckel and A. D. Stone, Nature (London) **385**, 45 (1997).
[11] V. Zharnitsky, Phys. Rev. Lett. **75**, 4393 (1995).
[12] K. M. Frahm and D. L. Shepelyansky, Phys. Rev. Lett. **78**, 1440 (1997).
[13] Y. M. Blanter, A. D. Mirlin, and B. A. Muzykantskii, Phys. Rev. Lett. **80**, 4161 (1998).
[14] T. Papenbrock and T. Prosen, Phys. Rev. Lett. **84**, 262 (2000).
[15] N. Friedman, L. Khaykovich, R. Ozeri, and N. Davidson, Phys. Rev. A **61**, 031403(R) (2000).
[16] H. E. Lehtihet and B. N. Miller, Physica (Amsterdam) **21D**, 93 (1986).
[17] P. H. Richter, H.-J. Scholz, and A. Wittek, Nonlinearity **3**, 45 (1990).
[18] T. Szeredi and D. A. Goodings, Phys. Rev. E **48**, 3518 (1993).
[19] S. Chu, Science **253**, 861 (1991).
[20] T. Szeredi and D. A. Goodings, Phys. Rev. Lett. **69**, 1640 (1992).
[21] C. Rouvinez and U. Smilansky, J. Phys. A **28**, 77 (1995).